Boundary layer thickness effects of the hydrodynamic instability along an impedance wall

EINDHOVEN UNIVERSITY OF TECHNOLOGY
Department of Mathematics and Computer Science

CASA-Report 10-69
November 2010

Boundary layer thickness effects of the hydrodynamic instability along an impedance wall

by

S.W. Rienstra, M. Darau

Centre for Analysis, Scientific computing and Applications
Department of Mathematics and Computer Science
Eindhoven University of Technology
P.O. Box 513
5600 MB Eindhoven, The Netherlands
ISSN: 0926-4507

Boundary Layer Thickness Effects of the Hydrodynamic Instability along an Impedance Wall

SJOERD W. RIENSTRA AND MIRELA DARAU

Department of Mathematics and Computer Science,
Eindhoven University of Technology,
P.O. Box 513, 5600 MB Eindhoven, The Netherlands

(Received 15 November 2010)

The Ingard-Myers condition, modelling the effect of an impedance wall under a mean flow by assuming a vanishingly thin boundary layer, is known to lead to an ill-posed problem in time-domain. By analysing the stability of a linear-then-constant mean flow over a mass-spring-damper liner in a 2D incompressible limit, we show that the flow is absolutely unstable for h smaller than a critical h_c and convectively unstable or stable otherwise. This critical h_c is by nature independent of wave length or frequency and is a property of liner and mean flow only. An analytical approximation of h_c is given, which is complemented by a contourplot covering all parameter values. For an aeronautically relevant example, h_c is shown to be extremely small, which explains why this instability has never been observed in industrial practice. A systematically regularised boundary condition, to replace the Ingard-Myers condition, is proposed that retains the effects of a finite h, such that the stability of the approximate problem correctly follows the stability of the real problem.

Key Words: Aeroacoustics, Boundary layer stability, Impedance wall

---

CONTENTS

1. Introduction

The problem we address is primarily a modelling problem, as we aim to clarify why a seemingly very thin mean flow boundary layer cannot be neglected. At the same time, the physical insight we provide may help to interpret recent experimental results.

Consider a liner of impedance $Z(\omega)$ at a wall along a main flow (U_0, ρ_0, c_0) with boundary layer of thickness h and acoustic waves of typical wavelength λ. At the wall, with vanishing mean flow velocity, the impedance relates the Fourier transformed pressure $\hat{p}(\omega)$ and normal velocity component $\hat{\boldsymbol{v}}(\omega)\cdot\boldsymbol{n}$ in the following way (see Hubbard 1995)

$$\hat{p} = Z\,(\hat{\boldsymbol{v}}\cdot\boldsymbol{n})$$

(where normal vector $\boldsymbol{n}$ points into the wall). This, however, is not a convenient boundary condition when the mean flow boundary layer is thin and the *effective* mean flow model is one with slip along the wall. In such a case the Ingard-Myers model (see Ingard 1959; Myers 1980; Eversman & Beckemeyer 1972; Tester 1973b) utilizes the fact that if $h \ll \lambda$, the sound waves don't see any difference between a finite boundary layer and a vortex sheet, so that the limit $h\to 0$ can be taken, resulting into the celebrated Ingard boundary condition (see Ingard 1959) for mean flow along a straight wall in (say) x-direction

$$\mathrm{i}\omega\,(\hat{\boldsymbol{v}}\cdot\boldsymbol{n}) = \left[\mathrm{i}\omega + U_0\frac{\partial}{\partial x}\right]\left(\frac{\hat{p}}{Z}\right)$$

or its generalisation by Myers (1980) for mean flow along a curved wall

$$\mathrm{i}\omega\,(\hat{\boldsymbol{v}}\cdot\boldsymbol{n}) = \left[\mathrm{i}\omega + \boldsymbol{V}_0\cdot\nabla - \boldsymbol{n}\cdot\left(\boldsymbol{n}\cdot\nabla\boldsymbol{V}_0\right)\right]\left(\frac{\hat{p}}{Z}\right).$$

It is clear that both conditions are extremely useful for numerical calculations in those cases where the boundary layer is indeed negligible.

For a long time, however, there have been doubts (see Tester 1973a; Rienstra 2003; Rienstra & Tester 2008) about a particular wave mode that exists along a lined wall with flow and the Ingard-Myers condition. This mode has some similarities with the Kelvin-Helmholtz instability of a free vortex sheet (see Rienstra 2007) and may therefore represent an instability, although the analysis is mathematically subtle (see Brambley & Peake 2006, 2008; Brambley 2008, 2009).

Since there was little or no indication that this instability was genuine, the problem seemed to be of minor practical importance, at least for calculations in frequency domain. However, once we approach the problem in time domain such that numerical errors generate perturbations of every frequency, it appears to our modeller's dislike that the instability is at least in the model very real. The flow appears to be absolutely unstable (see Chevaugeon, Remacle & Gallez 2006; Brambley & Peake 2006) and in fact it is worse: it is ill-posed, as Brambley showed (see Brambley 2009). Still, this absolute instability has not (see Jones 2007) or at least practically not (see Bauer & Chapkis 1977) been reported in industrial reality, and only very rarely experimentally (see Brandes & Ronneberger 1995; Aurégan, Leroux & Pagneux 2005; Aurégan & Leroux 2008; Marx, Aurégan, Baillet & Valière 2009) under special conditions. Although there is little doubt that the limit $h\to 0$ is correct, there must be something wrong in our modelling assumptions. In particular, there must be a very small length scale in the problem, other than λ, on which h scales at the onset of instability. This is what we will consider here.

The present paper consists of three parts.

Firstly, we will show that the above modelling anomaly may be explained, in an inviscid model with a vanishingly thin mean shear flow, by the existence of a (non-zero) critical boundary layer thickness h_c, such that the boundary layer is absolutely unstable for

$0 < h < h_c$ and not absolutely unstable (possibly convectively unstable) for $h > h_c$. It appears that for any industrially common configuration, h_c is very small. (We were originally inspired (see Rienstra & Vilenski 2008) for the concept of a critical thickness by the results of Michalke (1965, 1984) for the spatially unstable free shear layer, but it should be noted that an absolute instability is a more complex phenomenon.)

Secondly, we will make an estimate in analytic form of h_c as a function of the problem parameters. This will be valid for a parameter range that includes the industrially interesting cases. A contourplot relating the three dimensionless parameter groups completes the picture for all parameter values.

Thirdly, we will propose a corrected or regularised "Ingard-Myers" boundary condition, that replaces the boundary layer (like the Ingard-Myers limit) but includes otherwise neglected terms that account for the finite boundary layer thickness effects. This new boundary condition is physically closer to the full problem and predicts (more) correctly stable and unstable behaviour.

2. The problem

2.1. *Description*

An inviscid 2D parallel mean flow $U_0(y)$ (figure 1), with uniform mean pressure p_0 and density ρ_0, and small isentropic perturbations

$$u = U_0 + \tilde{u},\ v = \tilde{v},\ p = p_0 + \tilde{p},\ \rho = \rho_0 + \tilde{\rho}, \tag{2.1}$$

satisfies the usual linearised Euler equations given by

$$\begin{gathered}\frac{1}{\rho_0 c_0^2}\left(\frac{\partial \tilde{p}}{\partial t} + U_0\frac{\partial \tilde{p}}{\partial x}\right) + \frac{\partial \tilde{u}}{\partial x} + \frac{\partial \tilde{v}}{\partial y} = 0,\\ \frac{\partial \tilde{u}}{\partial t} + U_0\frac{\partial \tilde{u}}{\partial x} + \frac{\mathrm{d}U_0}{\mathrm{d}y}\tilde{v} + \frac{1}{\rho_0}\frac{\partial \tilde{p}}{\partial x} = 0,\\ \frac{\partial \tilde{v}}{\partial t} + U_0\frac{\partial \tilde{v}}{\partial x} + \frac{1}{\rho_0}\frac{\partial \tilde{p}}{\partial y} = 0.\end{gathered} \tag{2.2}$$

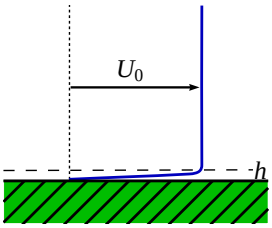

FIGURE 1. Mean flow.

where c_0 is the sound speed and $(\partial_t + U_0\partial_x)(\tilde{p} - c_0^2\tilde{\rho}) = 0$. When we consider waves of the type

$$\tilde{p}(x,y,t) = \frac{1}{2\pi}\int_{-\infty}^{\infty}\breve{p}(x,y;\omega)\,\mathrm{e}^{\mathrm{i}\omega t}\,\mathrm{d}\omega = \frac{1}{4\pi^2}\iint_{-\infty}^{\infty}\hat{p}(y;\alpha,\omega)\,\mathrm{e}^{\mathrm{i}\omega t - \mathrm{i}\alpha x}\,\mathrm{d}\alpha\mathrm{d}\omega, \tag{2.3}$$

(similarly for $\tilde{u}, \tilde{v}$), the equations become

$$\begin{gathered}\frac{\mathrm{i}(\omega - \alpha U_0)\hat{p}}{\rho_0 c_0^2} - \mathrm{i}\alpha\hat{u} + \frac{\mathrm{d}\hat{v}}{\mathrm{d}y} = 0,\\ \mathrm{i}(\omega - \alpha U_0)\hat{u} + \frac{\mathrm{d}U_0}{\mathrm{d}y}\hat{v} - \frac{\mathrm{i}\alpha}{\rho_0}\hat{p} = 0,\\ \mathrm{i}(\omega - \alpha U_0)\hat{v} + \frac{1}{\rho_0}\frac{\mathrm{d}\hat{p}}{\mathrm{d}y} = 0.\end{gathered} \tag{2.4}$$

They may be further reduced to a form of the Pridmore-Brown equation (see Pridmore-Brown 1958) by eliminating $\hat{v}$ and $\hat{u}$

$$\frac{\mathrm{d}^2\hat{p}}{\mathrm{d}y^2} + \frac{2\alpha\frac{\mathrm{d}}{\mathrm{d}y}U_0}{\omega - \alpha U_0}\frac{\mathrm{d}\hat{p}}{\mathrm{d}y} + \left(\frac{(\omega - \alpha U_0)^2}{c_0^2} - \alpha^2\right)\hat{p} = 0. \tag{2.5}$$

At $y = 0$ we have a uniform impedance boundary condition

$$-\frac{\hat{p}(0)}{\hat{v}(0)} = Z(\omega). \tag{2.6}$$

We select solutions of surface wave type, by assuming exponential decay for $y \to \infty$.

The mean flow is typically uniform everywhere, equal to U_∞, except for a thin boundary layer of thickness h. We look for frequency (ω) and wavenumber (α) combinations that allow a solution. The stability of this solution will be investigated as a function of the problem parameters. In particular we will be interested in the critical thickness $h = h_c$ below which the flow becomes absolutely unstable.

2.2. *Dimension analysis and scaling*

As the frequency and wave number at which the absolute instability first appears is part of the problem, it is clear that h_c does not depend on ω or α. As a consequence, the Ingard-Myers limit, $h \to 0$, based on $h/\lambda \ll 1$ (λ a typical acoustic wavelength) is not applicable to the instability problem. Furthermore, since the associated surface wave (see Rienstra 2003, eqs. (12)-(13)) is of hydrodynamic nature and inherently incompressible, h_c is only weakly depending on sound speed c_0, with p_0 also playing no role anymore. As there are no other length scales in the fluid, h_c must scale on an inherent length scale of the liner. Suppose we have a liner of mass-spring-damper type with resistance R, inertance m and stiffness K, then

$$Z(\omega) = R + \mathrm{i}\omega m - \mathrm{i}K/\omega. \tag{2.7a}$$

If the liner is built from Helmholtz resonators (see Rienstra 2006) of cell depth L and

$$Z(\omega) = R + \mathrm{i}\omega\tilde{m} - \mathrm{i}\rho_0 c_0 \cot(\omega L/c_0), \tag{2.7b}$$

and designed to work near the first cell resonance frequency (where $\mathrm{Im}(Z) = 0$), then $\omega L/c_0$ is small for the relevant frequency range, and we can approximate the Helmholtz resonator by a mass-spring-damper system with $K \simeq \rho_0 c_0^2/L$ and $m = \tilde{m} + \frac{1}{3}\rho_0 L$ (see Richter 2009). Thus, we have 6 parameters $(h_c, \rho_0, U_\infty, R, m, K)$ and 3 dimensions (m, kg, s), so it follows from Buckingham's theorem that our problem has three dimensionless numbers, for example

$$\frac{R}{\rho_0 U_\infty},\ \frac{mK}{\rho_0^2 U_\infty^2},\ \frac{Kh_c}{\rho_0 U_\infty^2}. \tag{2.8}$$

Later (section 3.3) we will see that a proper reference length scale for h_c, i.e. one that preserves its order of magnitude, is a more complicated combination of these parameters. More specifically, we will find that we can write, for a function $H = O(1)$,

$$h_c = \left(\frac{\rho_0 U_\infty}{R}\right)^2 U_\infty \sqrt{\frac{m}{K}}\, H\left(\frac{R}{\rho_0 U_\infty}, \frac{\sqrt{mK}}{\rho_0 U_\infty}\right). \tag{2.9}$$

However, at this stage nothing can be said about this scaling yet. Since nondimensionalisation on arbitrary scaling values is not particularly useful, at least not here, we therefore deliberately leave the problem in *dimensional* form.

2.3. *The model: incompressible linear-then-constant shear flow*

As the stability problem is essentially incompressible, we consider the incompressible limit, where $\omega/\alpha, U_0 \ll c_0$. Then the Pridmore-Brown equation reduces to

$$\frac{\mathrm{d}^2\hat{p}}{\mathrm{d}y^2} + \frac{2\alpha\frac{\mathrm{d}}{\mathrm{d}y}U_0}{\omega - \alpha U_0}\frac{\mathrm{d}\hat{p}}{\mathrm{d}y} - \alpha^2\hat{p} = 0. \tag{2.10}$$

If we assume a linear-then-constant velocity profile of thickness h

$$U_0(y) = \begin{cases} \dfrac{y}{h}U_\infty & \text{for} \quad 0 \leqslant y \leqslant h \\ U_\infty & \text{for} \quad h \leqslant y < \infty \end{cases} \tag{2.11}$$

we have an exact solution for our problem. For $y \geqslant h$ we have

$$\hat{p} = A\,\mathrm{e}^{-|\alpha|y}, \quad \text{where} \quad |\alpha| = \operatorname{sgn}(\operatorname{Re}\alpha)\alpha. \tag{2.12}$$

Other representations of $|\alpha|$ are $\sqrt{\alpha^2}$ or $\sqrt{\mathrm{i}\alpha}\sqrt{-\mathrm{i}\alpha}$ with principal square roots assumed for $\sqrt{\cdot}$ in all cases. $|\alpha|$ is the generalisation of the real absolute value function which is analytic in the right and in the left complex halfplane. It has discontinuities along $(-\mathrm{i}\infty, 0)$ and $(0, \mathrm{i}\infty)$, which correspond with the branch cuts of the square roots. The notation $|\alpha|$ is very common in this kind of problems (see Lingwood & Peake 1999; Peake 1997, 2002), but of course should not be confused with the complex modulus of α. However, in this paper the complex modulus does not occur.

In the shear layer region $(0, h)$ we have

$$\hat{p}(y) = C_1\,\mathrm{e}^{\alpha y}(h\omega - \alpha y U_\infty + U_\infty) + C_2\,\mathrm{e}^{-\alpha y}(h\omega - \alpha y U_\infty - U_\infty) \tag{2.13a}$$

$$\hat{u}(y) = \frac{\alpha h}{\rho_0}(C_1\,\mathrm{e}^{\alpha y} + C_2\,\mathrm{e}^{-\alpha y}) \tag{2.13b}$$

$$\hat{v}(y) = \frac{\mathrm{i}\alpha h}{\rho_0}(C_1\,\mathrm{e}^{\alpha y} - C_2\,\mathrm{e}^{-\alpha y}). \tag{2.13c}$$

This last solution is due to Rayleigh (see Drazin & Reid 2004), but has been used in a similar context of stability of flow along a flexible wall by Lingwood & Peake (1999).

2.4. *The dispersion relation*

When we apply continuity of pressure and particle displacement (which is, in this case, equivalent to continuity of normal velocity, since the mean flow is continuous) at the interface $y = h$, and the impedance boundary condition at $y = 0$, we obtain the necessary relation between ω and α for a solution to exists. This is the dispersion relation of the waves of interest, given by

$$0 = D(\alpha, \omega) = Z(\omega) + \frac{\mathrm{i}\rho_0}{\alpha h} \cdot \frac{(h\omega - U_\infty)(\alpha h\Omega + |\alpha|(h\Omega + U_\infty))\,\mathrm{e}^{\alpha h} + (h\omega + U_\infty)(\alpha h\Omega - |\alpha|(h\Omega - U_\infty))\,\mathrm{e}^{-\alpha h}}{(\alpha h\Omega + |\alpha|(h\Omega + U_\infty))\,\mathrm{e}^{\alpha h} - (\alpha h\Omega - |\alpha|(h\Omega - U_\infty))\,\mathrm{e}^{-\alpha h}} \tag{2.14}$$

where

$$\Omega = \omega - \alpha U_\infty. \tag{2.15}$$

3. Stability analysis

3.1. *Briggs-Bers analysis*

We are essentially interested in any possible *spurious* absolutely unstable behaviour of our model, as this has by far the most dramatic consequences for numerical calculation in time-domain (see Chevaugeon, Remacle & Gallez 2006). Of course, it is also of interest if the instability is physically genuine, like may be the case in the papers of Brandes & Ronneberger (1995); Aurégan, Leroux & Pagneux (2005); Aurégan & Leroux (2008); Marx, Aurégan, Baillet & Valière (2009), but for aeronautical applications this is apparently very rare (see Bauer & Chapkis 1977; Jones 2007).

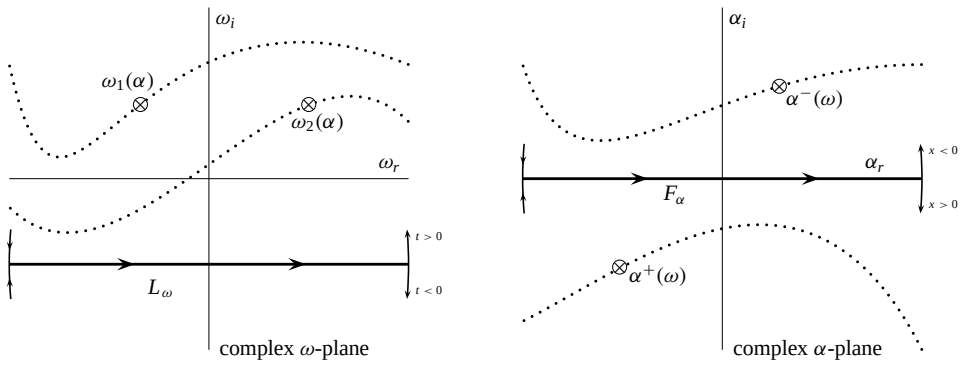

FIGURE 2. Paths of integration in ω-plane and in α-plane between *sketched* possible behaviour of poles.

To identify absolutely unstable behaviour we have to search for causal modes with vanishing group velocity (and an additional "pinching" requirement). For this we follow the method, originally developed by Briggs (1964) and Bers (1983) for plasma physics applications, but subsequently widely applied for fluid mechanical and aeroacoustical applications (see Huerre & Monkewitz 1985; Peake 1997; Lingwood & Peake 1999; Peake 2002; Brambley & Peake 2006, 2008).

If the impulse response of the system may be represented generically by a double Fourier integral

$$\Psi(x,y,t) = \frac{1}{(2\pi)^2}\int_{L_\omega}\int_{F_\alpha}\frac{\varphi(y)}{D(\alpha,\omega)}\,\mathrm{e}^{\mathrm{i}\omega t-\mathrm{i}\alpha x}\,\mathrm{d}\alpha\mathrm{d}\omega, \tag{3.1}$$

the integration contours L_ω and F_α (figure 2) have to be located in domains of *absolute convergence* in the complex ω- and α-planes:

- For the ω-integral, L_ω should be below any poles $\omega_j(\alpha)$ given by $D(\alpha,\omega)=0$, where $\alpha\in F_\alpha$. This is due to causality that requires $\Psi=0$ for $t<0$ and the $\mathrm{e}^{\mathrm{i}\omega t}$-factor.
- For the α-integral, F_α should be in a strip along the real axis between the left and right running poles, $\alpha^-(\omega)$ and $\alpha^+(\omega)$ given by $D(\alpha,\omega)=0$, for $\omega\in L_\omega$.

The main idea is that we exploit the freedom we have in the location of L_ω and F_α. The first step is that we check that there exists a minimum imaginary part of the possible ω_j:

$$\omega_{min} = \min_{\alpha\in\mathbb{R}}\left[\mathrm{Im}\,\omega_j(\alpha)\right]. \tag{3.2}$$

This is relatively easy for a mass-spring-damper impedance, because the dispersion relation is equivalent to a third order polynomial in ω with just 3 solutions, which can be traced without difficulty. See figure 3 for a typical case (note that it suffices to consider $\mathrm{Re}(\alpha)>0$ because of the symmetry of D). There is a minimum imaginary part, so Briggs-Bers' method is applicable. Since $\omega_{min}<0$, the flow is unstable.

Then we consider poles α^+ and α^- in the α plane, and plot $\alpha^\pm(\omega)$-images of the line $\mathrm{Im}(\omega)=c\geqslant\omega_{min}$. Note that while c is increased, contour F_α has to be deformed in order not to cross the poles, but always via the origin because of the branch cuts along the imaginary axis. As c is increased, α^+ and α^- approach each other until they collide for $\omega=\omega^*$ into $\alpha=\alpha^*$, where the F_α-integration contour is pinched, unable to be further deformed; see figure 4 for a typical case. If $\mathrm{Im}(\omega^*)<0$, resp. >0, then (ω^*,α^*) corresponds to an *absolute*, resp. *convective* instability. Since two solutions of $D(\alpha,\omega)=0$ coalesce, they satisfy the additional equation $\frac{\partial}{\partial\alpha}D(\alpha,\omega)=0$, so (ω^*,α^*) must satisfy the

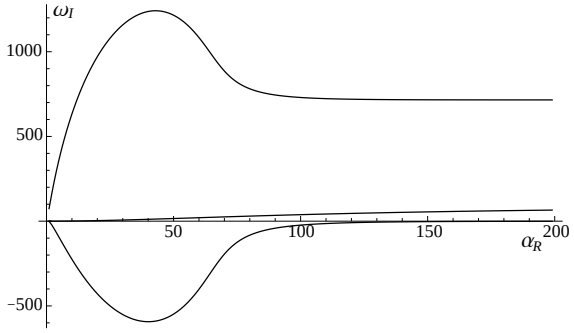

FIGURE 3. Plots of $\mathrm{Im}(\omega_j(\alpha))$ for $\alpha \in \mathbb{R}$. All have a minimum imaginary part so Briggs-Bers' method is applicable. ($\rho_0 = 1.22$, $U_\infty = 82$, $h = 0.01$, $R = 100$, $m = 0.1215$, $K = 8166$.)

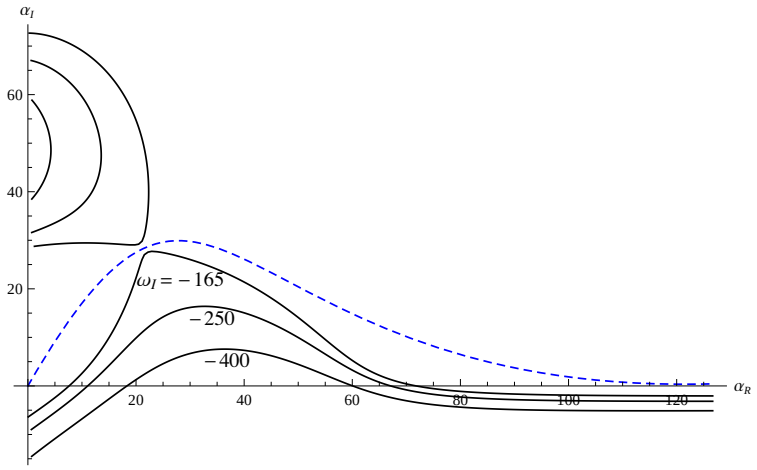

FIGURE 4. Plots of poles $\alpha^+(\omega)$ and $\alpha^-(\omega)$ for varying $\mathrm{Im}(\omega) = c$ until they collide for $c = -165$. So in this example (with $\rho_0 = 1.22$, $U_\infty = 82$, $h = 0.01$, $R = 100$, $m = 0.1215$, $K = 8166$) the flow is absolutely unstable.

two equations, and in addition it must be the collision of a right- and a left-running mode (this can be checked on the plots in the α-plane).

3.2. *A typical example from aeronautical applications*

As a typical aeronautical example we consider a low Mach number mean flow $U_\infty = 60$ m/s, $\rho_0 = 1.225$ kg/m^3 and $c_0 = 340$ m/s, with an impedance of Helmholtz resonator type (see Rienstra 2006)

$$Z(\omega) = R + \mathrm{i}\omega\tilde{m} - \mathrm{i}\rho_0 c_0 \cot\Big(\frac{\omega L}{c_0}\Big) \approx R + \mathrm{i}\omega\left(\tilde{m} + \frac{1}{3}\rho_0 L\right) - \mathrm{i}\frac{\rho_0 c_0^2}{\omega L}, \tag{3.3}$$

which is chosen such that $R = 2\rho_0 c_0 = 833$ kg/m^{2}s, cell depth $L = 3.5$ cm and $\tilde{m}/\rho_0 = 20$ mm, leading to $K = 4.0 \cdot 10^6$ kg/m^{2}s^2 and $m = 0.039$ kg/m^2.

When we vary the boundary layer thickness h, and plot the imaginary part (= minus growth rate) of the found frequency ω^*, we see that once h is small enough, the instability becomes absolute. See figure 5. We call the value of h where $\mathrm{Im}(\omega^*) = 0$ the critical thickness h_c, because for any $h < h_c$ the instability is absolute. Note that $\mathrm{Im}(\omega^*) \to -\infty$ for $h \downarrow 0$ so the growth rate becomes unbounded for $h = 0$, which confirms the ill-posedness of the Ingard-Myers limit, as observed by Brambley (2009). For the present example, the

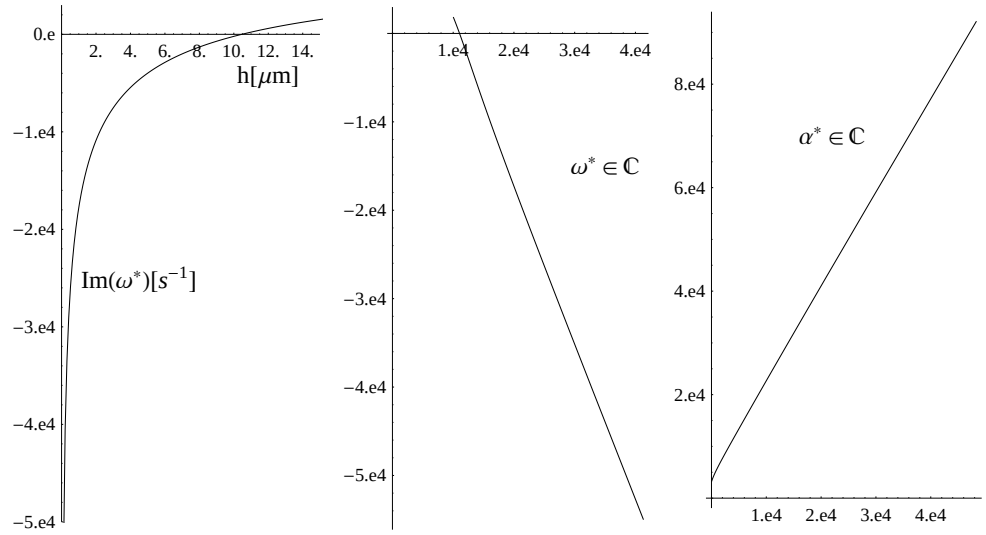

FIGURE 5. Growth rate $\mathrm{Im}(\omega^*)$ against h of potential absolute instability at vanishing group velocity (pinch point) is plotted together with the corresponding complex frequency ω^* and wave number α^*.

critical thickness h_c appears to be extremely small, namely

$$h_c = 10.5 \cdot 10^{-6}\mathrm{m} = 10.5\ \mu\mathrm{m},\ \text{with}\ \omega^* = 11023.4\ \mathrm{s}^{-1},\ \alpha^* = 364.887 + \mathrm{i}4188.99\ \mathrm{m}^{-1}. \quad (3.4)$$

This result is typical. For other industrially relevant liner top plate porosities and thicknesses (leading to other values of $\tilde{m}$), we find similar values, namely $h_c = 8.5\ \mu$m for $\tilde{m}/\rho_0 = 10$ mm, and $h_c = 13.6\ \mu$m for $\tilde{m}/\rho_0 = 40$ mm.

It is clear that these values are smaller than any practical boundary layer thickness, so a real flow will not be absolutely unstable, in contrast to any model that adopts the Ingard-Myers limit, even though this is at first sight a very reasonable assumption if the boundary layer is only a fraction of any relevant acoustic wave length.

3.3. *Approximation for large $R/\rho_0 U_\infty$ and large $\sqrt{mK}/R$*

Insight is gained into the functional relationship between h_c and the other problem parameters by considering relevant asymptotic behaviour. If the wall has a high "hydrodynamic" resistance, i.e. $r = R/\rho_0 U_\infty \gg 1$ and a high quality factor of the resonator, i.e. $\sqrt{mK}/R = O(r)$, then the inherent scalings for h_c appear to be $m/\rho_0 h_c = O(r^4)$, $\alpha h_c = O(r^{-1})$ and $\omega h_c/U_\infty = O(r^{-2})$, such that we get to leading order from $D(\alpha,\omega) = 0$ and $D_\alpha(\alpha,\omega) = 0$

$$\begin{gathered} \mathrm{i}\left(m\omega - \frac{K}{\omega}\right) + \left(R + \mathrm{i}\rho_0 U_\infty \frac{\alpha h_c}{\frac{\omega h_c}{U_\infty} - \alpha^2 h_c^2}\right) + \cdots = 0, \\ \left(\frac{\mathrm{i}}{\frac{\omega h_c}{U_\infty} - \alpha^2 h_c^2} + \frac{2\mathrm{i}\alpha^2 h_c^2}{\left(\frac{\omega h_c}{U_\infty} - \alpha^2 h_c^2\right)^2}\right) + \cdots = 0 \end{gathered} \quad (3.5)$$

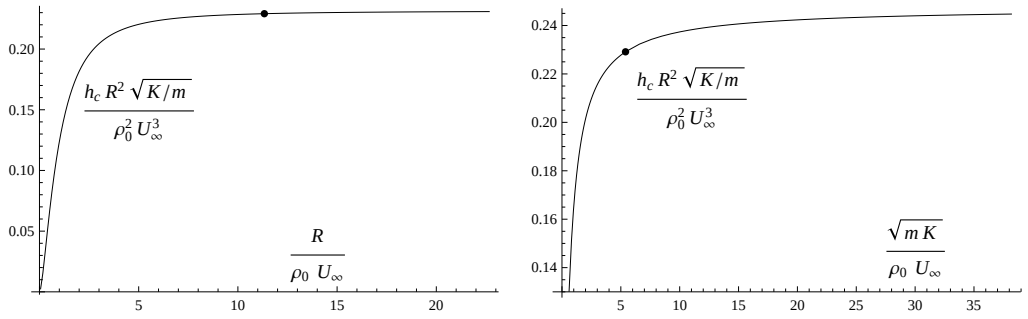

FIGURE 6. Variation in R and $\sqrt{mK}$ with $U_\infty = 60$, $\rho_0 = 1.225$, $K = 4 \cdot 10^6$, $R = 2\rho_0 c_0$ and $m = 0.039$. The dot corresponds with the conditions of example 3.2.

With the condition that ω is real, we have

$$\omega \simeq \sqrt{\frac{K}{m}}, \qquad \frac{\omega h_c}{U_\infty} + (\alpha h_c)^2 \simeq 0, \qquad \frac{R}{\rho_0 U_\infty} - \frac{\mathrm{i}}{2\alpha h_c} \simeq 0, \tag{3.6}$$

resulting into the approximate relation

$$h_c \simeq \frac{1}{4}\left(\frac{\rho_0 U_\infty}{R}\right)^2 U_\infty \sqrt{\frac{m}{K}}. \tag{3.7}$$

This is confirmed by the numerical results given in figures 6 and 7. Here, dimensionless quantity

$$\frac{h_c R^2 \sqrt{K/m}}{\rho_0^2 U_\infty^3} = H\left(\frac{R}{\rho_0 U_\infty}, \frac{\sqrt{mK}}{\rho_0 U_\infty}\right) \tag{3.8}$$

(the function H of equation 2.9) is plotted as a function of dimensionless parameters $R/\rho_0 U_\infty$ and $\sqrt{mK}/\rho_0 U_\infty$. In figure 6 one parameter is varied while the other is held fixed at the conditions of the example in section 3.2, and vice versa. An even more comprehensive result is given in figure 7 where a contourplot of H is given. From (3.7) we know that H becomes asymptotically equal to 0.25. Indeed, we see that for a rather large parameter range - including the above example (indicated by a dot) - H is found between 0.2 and 0.25. So expression (3.7) appears to be an good estimate of h_c for R, K and m not too close to zero.

4. A regularised boundary condition

4.1. *Approximations for small αh*

If we carefully consider the *third* order approximations of the exponentials for $\alpha h \to 0$, i.e. $\mathrm{e}^{\pm\alpha h} \simeq 1 \pm \alpha h + \frac{1}{2}(\alpha h)^2 \pm \frac{1}{6}(\alpha h)^3$, of both the numerator and denominator of the dispersion relation $D(\alpha, \omega) = 0$, then collect powers of αh up to $O(\alpha h)$, with $\omega h/U_\infty = O(\alpha h)$, and ignore higher order terms, we find

$$Z(\omega) \simeq \frac{\rho_0}{\mathrm{i}} \cdot \frac{\Omega^2 + |\alpha|(\omega\Omega + \frac{1}{3}U_\infty^2 \alpha^2)h}{|\alpha|\omega + \alpha^2 \Omega h} \tag{4.1}$$

where $\Omega = \omega - \alpha U_\infty$. This expansion is obviously not unique. We can multiply numerator and denominator by any suitable function of αh, re-expand, and obtain a different, but asymptotically equivalent form. For example, we can multiply by $\mathrm{e}^{-|\alpha|h\theta} / \mathrm{e}^{-|\alpha|h\theta}$ and

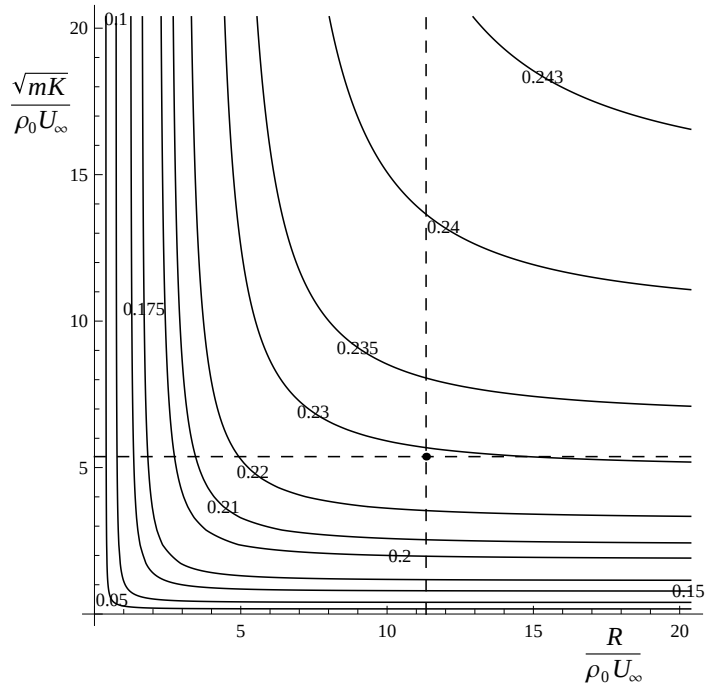

FIGURE 7. Contour plot of $h_c R^2\sqrt{K/m}/(\rho_0^2 U_\infty^3)$ as a function of $R/\rho_0 U_\infty$ and $\sqrt{mK}/\rho_0 U_\infty$. The dashed lines correspond to figure 6. The dot corresponds with the conditions of example 3.2.

obtain after re-expanding numerator and denominator

$$Z(\omega) \simeq \frac{\rho_0}{\mathrm{i}} \cdot \frac{\Omega^2 + |\alpha|((1-\theta)\omega^2 - (1-2\theta)\omega\alpha U_\infty + (\frac{1}{3}-\theta)\alpha^2 U_\infty^2)h}{|\alpha|\omega + \alpha^2(\Omega - \theta\omega)h}$$

It is not immediately clear if there is a practically preferable choice of θ, but a particularly pleasing result seems to be obtained by $\theta = \frac{1}{3}$. For this choice the coefficient of the highest power of α in the numerator is reduced to 2 and the approximate solutions are remarkably close to the "exact" ones, at least in the industrial example considered here, as will shown below (section 4.3, figure 8). So in the following we will continue with the approximation

$$Z(\omega) \simeq \frac{\rho_0}{\mathrm{i}} \cdot \frac{\Omega^2 + |\alpha|\omega(\frac{2}{3}\omega - \frac{1}{3}\alpha U_\infty)h}{|\alpha|\omega + \alpha^2(\Omega - \frac{1}{3}\omega)h} = \frac{\mathrm{i}\Omega - \rho_0 \dfrac{-|\alpha|}{\mathrm{i}\Omega\rho_0}\mathrm{i}\omega\big(\frac{2}{3}\mathrm{i}\omega - \frac{1}{3}\mathrm{i}\alpha U_\infty\big)h}{\mathrm{i}\omega\dfrac{-|\alpha|}{\mathrm{i}\Omega\rho_0} + \dfrac{(-\mathrm{i}\alpha)^2}{\rho_0}h - \frac{1}{3}\mathrm{i}\omega\dfrac{-|\alpha|}{\mathrm{i}\Omega\rho_0}|\alpha|h}, \tag{4.2}$$

recast in a form convenient later.

4.2. *A modified Ingard-Myers boundary condition*

Although the approximation is for small αh, it should be noted that the behaviour for large α is such that the solutions of *this* approximate dispersion relation have exactly the same behaviour with respect to the stability as the solutions of the original $D(\alpha,\omega) = 0$ (see below). Not only are all modes $\omega_j(\alpha)$ bounded from below when $\alpha \in \mathbb{R}$, but also is the found h_c as a function of the problem parameters very similar to the "exact" one for the practical cases considered above. It therefore makes sense to consider an equivalent boundary condition that exactly produces this approximate dispersion relation and hence replaces the effect of the boundary layer (just like the Ingard-Myers limit) but now with

a *finite* h. If we include a small but non-zero h the ill-posedness and associated absolute instability can be avoided. Most importantly, this is without sacrificing the physics but, on the contrary, by restoring a little bit of the inadvertently neglected physics!

If we identify at $y = 0$

$$-\mathrm{i}\alpha\hat{p} \sim \frac{\partial}{\partial x}\breve{p}, \qquad \frac{-|\alpha|}{\mathrm{i}\Omega\rho_0}\hat{p} = (\hat{\boldsymbol{v}}\cdot\boldsymbol{n}), \qquad |\alpha|(\hat{\boldsymbol{v}}\cdot\boldsymbol{n}) \sim \frac{\partial}{\partial \boldsymbol{n}}(\breve{\boldsymbol{v}}\cdot\boldsymbol{n}), \tag{4.3}$$

for the normal vector $\boldsymbol{n}$ pointing *into* the surface, then we have a "corrected" or "regularised" Ingard-Myers boundary condition

$$Z(\omega) = \frac{\left(\mathrm{i}\omega + U_\infty\frac{\partial}{\partial x}\right)\breve{p} - h\rho_0\mathrm{i}\omega\left(\frac{2}{3}\mathrm{i}\omega + \frac{1}{3}U_\infty\frac{\partial}{\partial x}\right)(\breve{\boldsymbol{v}}\cdot\boldsymbol{n})}{\mathrm{i}\omega(\breve{\boldsymbol{v}}\cdot\boldsymbol{n}) + \dfrac{h}{\rho_0}\dfrac{\partial^2}{\partial x^2}\breve{p} - \frac{1}{3}h\mathrm{i}\omega\dfrac{\partial}{\partial \boldsymbol{n}}(\breve{\boldsymbol{v}}\cdot\boldsymbol{n})}, \tag{4.4}$$

which indeed reduces for $h = 0$ to the Ingard approximation, but now has the *physically correct* stability behaviour. (Note that the Myers generalisation for curved surfaces is far more complicated.)

Recently Brambley (2010) proposed a corrected Ingard boundary condition for cylindrical duct modes and smooth velocity profiles of compressible flows, derived from an approximate solution of matched expansion type for thin mean flow boundary layers, similar to the solution by Eversman & Beckemeyer (1972). At first sight, his results, when applied to a linear-then-constant profile, are not exactly in agreement with (4.1), but, as we pointed out before, these approximations are not unique, and to the best of our knowledge Brambley's and our forms are asymptotically equivalent (apart from an obvious 2D-3D difference). In particular, there is no difference due to compressibility effects because these are of higher order in αh.

4.3. *Stability behaviour of the approximate dispersion relation*

A way to study the well-posedness of the problem with the regularised boundary condition for a mass-spring-damper impedance is to verify the lower boundedness of $\mathrm{Im}(\omega)$ as a function of α. Since ω is continuous in α and finite everywhere, it is enough to consider the asymptotic behaviour to large real α while keeping the other length scales fixed. Equation (4.2) leads to a third order polynomial in ω. Using perturbation techniques for small $1/\alpha$ we find that two of the roots behave to leading order as

$$\omega = \mathrm{i}\frac{R}{2m} \pm \mathrm{i}\frac{1}{2m}\sqrt{R^2 - 4Km} + O(1/\alpha)$$

while the third one is given by

$$\omega = \frac{3}{2}\alpha U_\infty - \mathrm{sgn}(\alpha)\left(\frac{9}{4} + \frac{\rho_0 h}{m}\right)\frac{U_\infty}{h} + O(1/\alpha)$$

So for two of the three solutions, the imaginary part of ω tends to some constant values, while the third is $O(1/\alpha)$ and so approaches zero. This is confirmed by figure 8 for the same parameter values as in figure 3. Such being the case, the Briggs-Bers' method is applicable.

If, for the proposed boundary condition (4.4), we vary again h and plot for the example of section 3.2 (as in figure 5) the imaginary part of the frequency ω^*, with $\mathrm{Im}(\omega^*) = 0$, we find practically the same results as for the "exact value" (figure 9). Also the value h_c for which the flow turns from convectively unstable to absolutely unstable is very close to the "exact" value.

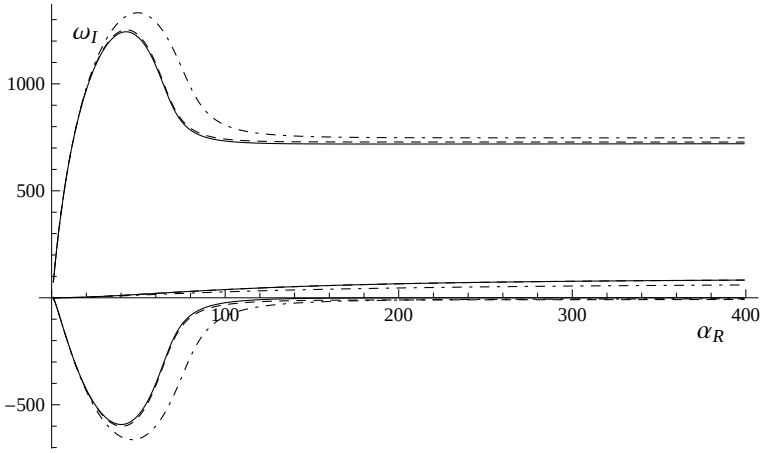

FIGURE 8. Plots of $\mathrm{Im}(\omega_j(\alpha))$ for $\alpha \in \mathbb{R}$ for the exact (solid) and the approximate ($\theta = \frac{1}{3}$ dashed; $\theta = 0$ dot-dashed) dispersion relation. The parameter values are as in figure 3.

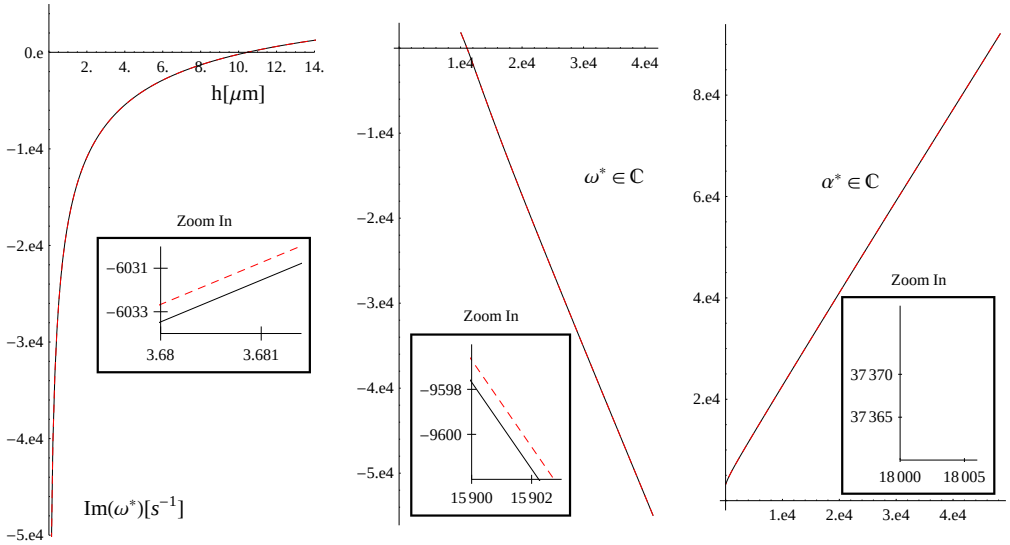

FIGURE 9. Comparison for the exact (solid) with approximate (dashed) solution using (4.4): growth rate $\mathrm{Im}(\omega^*)$ against h of potential absolute instability at vanishing group velocity (pinch point) is plotted together with the corresponding complex frequency ω^* and wave number α^*.

A rather good agreement was also found for the approximation that corresponds with $\theta = 0$ (equation 4.1) but the present high accuracy is definitely due to the particular choice of $\theta = \frac{1}{3}$ (equation 4.2). See for example figure 8 where exact results are compared with the approximations for $\theta = 0$ and $\theta = \frac{1}{3}$. A similar comparison in figure 9 is not given although it would have led to the same conclusion. The typical error of $O(10^2)$ of the $\theta = 0$ approximation would be too small for the large graphs, but too big for the zoom-ins, to be visible.

From these results we think it is reasonable to assume that the stability behaviour of the regularised Ingard-Myers boundary condition is for the industrially relevant cases the same as for the finite boundary layer model studied here.

5. Conclusions

The stability of a mass-spring-damper liner with incompressible flow with linear-then-constant velocity profile is analysed. The flow is found to be absolutely unstable for small but finite boundary layer h, say $0 < h < h_c$. In the limit of $h \downarrow 0$ the growth rate tends to infinity and the flow may be called *hyper-unstable*, which confirms the ill-posedness of the Ingard-Myers limit. These results in the incompressible assumption are confirmed in the recent paper by Brambley (2010) for compressible flows.

The critical thickness h_c is a property of flow and liner, and has no relation with any acoustic wavelength. So neglecting the effect of a finite h (as is done when applying the Ingard-Myers limit) can not be justified by comparing h with a typical acoustic wavelength. An explicit approximate formula for h_c is formulated, which incidentally shows that the characteristic length scale for h_c is not easily guessed from the problem. This analytic result is completed by a contourplot giving h_c for all parameter values. Anticipating a weak dependence of h_c on Mach number and geometry, this result could be very useful for numerical simulations, to assess the order of magnitude of boundary layers that are not absolutely unstable.

In industrial practice h_c is much smaller than any prevailing boundary layer thicknesses, which explains why the absolute instability of the present kind has not yet been observed. Although apparently never observed in industrial practice, there may be a convective instability that remains too small to be measured (in all the examples we investigated we found for $h > h_c$ a convective instability). The fact that we found no stable cases may be due to the simplifications adopted for our model.

The very existence of this critical h_c emphasises that $h = 0$ is not an admissible modelling assumption, and a proper model (at least in time domain) will have to have a finite $h > h_c$ in some way. Therefore, a corrected "Ingard-Myers" condition, including h, is proposed which is not absolutely unstable for $h > h_c$. Since this is based on a 2D incompressible model with a linear velocity profile it goes without saying that some margin is to be taken when applied in a more realistic situation.

The linear profile has the great advantage of an exact solution, but of course the price to be paid is the absence of a critical layer singularity (see Campos, Oliveira & Kobayashi 1999), i.e. a singularity of the solution at $y = y_c$, where $\omega - \alpha U_0(y_c) = 0$. This is subject of ongoing research.

Acknowledgements

This paper is an adapted and extended version of the IUTAM 2010 Symposium on Computational Aero-Acoustics contribution (see Rienstra & Darau 2010).

We gratefully acknowledge that the present project is a result of the cooperation between the Eindhoven University of Technology (Netherlands), Department of Mathematics and Computer Science, and the West University of Timisoara (Romania), Faculty of Mathematics and Informatics, realised, supervised and guided by professors Robert R.M. Mattheij and Stefan Balint.

We thank professor Patrick Huerre for his advice and helpful suggestions on the stability analysis.

We thank Thomas Nodé-Langlois, Michael Jones, Edward Rademaker and Andrew Kempton for their help with choosing typical liner parameters.

We thank Ed Brambley for noting the apparent difference between his approximate dispersion relation and ours. It inspired us to utilise the non-uniqueness of these expansions and produce a better approximation.

REFERENCES

Aurégan, Y. Leroux, M. 2008 Experimental evidence of an instability over an impedance wall in a duct flow, *Journal of Sound and Vibration*, **317**, 432–439.

Aurégan, Y. Leroux, M. Pagneux, V. 2005 Abnormal behavior of an acoustical liner with flow, *Forum Acusticum, Budapest.*

Bauer, A.B. & Chapkis, R.L. 1977 Noise Generated by Boundary-Layer Interaction with Perforated Acoustic Liners, *Journal of Aircraft*, **14** (2), 157–160.

Bers, A. 1983 Space-Time Evolution of Plasma Instabilities – Absolute and Convective, *Handbook of Plasma Physics: Volume 1 Basic Plasma Physics*, edited by A.A. Galeev and R.N. Sudan, North Holland Publishing Company, Chapter 3.2, 451–517.

Brambley, E.J. & Peake, N. 2006 Surface-Waves, Stability, and Scattering for a Lined Duct with Flow, AIAA-2006-2688, *12th AIAA/CEAS Aeroacoustics Conference, 8-10 May 2006, Cambridge, MA.*

Brambley, E.J. & Peake, N. 2008 Stability and acoustic scattering in a cylindrical thin shell containing compressible mean flow, *Journal of Fluid Mechanics*, **602**, 403–426, 2008.

Brambley, E.J. 2008 Models for Acoustically-Lined Turbofan Ducts. AIAA 2008-2879, *14th AIAA/CEAS Aeroacoustics Conference, 5-7 May 2008, The Westin Bayshore Vancouver, Vancouver, Canada.*

Brambley, E.J. 2009 Fundamental problems with the model of uniform flow over acoustic linings, *Journal of Sound and Vibration*, **322**, 1026–1037, 2009.

Brambley, E.J. 2008 A well-posed modified Myers boundary condition. AIAA 2010-3942, *16th AIAA/CEAS Aeroacoustics Conference, June 7-9 2010, Stockholm, Sweden.*

Brandes, M. & Ronneberger, D. 1995 Sound amplification in flow ducts lined with a periodic sequence of resonators, AIAA-95-126, *1st AIAA/CEAS Aeroacoustics Conference, 12-15 June 1995, Munich, Germany.*

Briggs, R.J. 1964 Electron-Stream Interaction with Plasmas, *Monograph* no. 29, MIT Press, Cambridge Mass., 1964

Campos, L.M.B.C. Oliveira, J.M.G.S. & Kobayashi, M.H. 1999 On sound propagation in a linear shear flow, *Journal of Sound and Vibration*, **219** (5), 739–770.

Chevaugeon, N. Remacle, J.-F. & Gallez, X. 2006 Discontinuous Galerkin Implementation of the Extended Helmholtz Resonator Impedance Model in Time Domain, AIAA-2006-2569, *12th AIAA/CEAS Aeroacoustics Conference, 8-10 May 2006, Cambridge, MA*

Drazin, P.G. & Reid, W.H. 2004 *Hydrodynamic Stability*, Cambridge University Press, 2nd edition, 2004

Eversman, W. & Beckemeyer, R.J. 1972 Transmission of sound in ducts with thin shear layers-convergence to the uniform flow case, *Journal of the Acoustical Society of America*, **52** (1), 216–220.

Hubbard, H.H. 1995 *Aeroacoustics of Flight Vehicles: Theory and Practice. Volume 2: Noise Control*, Acoustical Society of America, Woodbury, NY.

Huerre, P. & Monkewitz, P.A. 1985 Absolute and convective instabilities in free shear layers, *Journal of Fluid Mechanics*, **159**, 151–168.

Ingard, K.U. 1959 Influence of Fluid Motion Past a Plane Boundary on Sound Reflection, Absorption, and Transmission, *Journal of the Acoustical Society of America* **31** (7), 1035–1036.

Jones, M.G. 2007 NASA Langley Research Center, private communication, 2007.

Lingwood, R.J. & Peake, N. 1999 On the causal behaviour of flow over an elastic wall, *Journal of Fluid Mechanics*, **396**, 319–344.

Marx, D. Aurégan, Y. Baillet, H. & J. Valière 2010 Evidence of hydrodynamic instability over a liner in a duct with flow,*Journal of Sound and Vibration*, **329**, 3798–3812.

Michalke, A. 1965 On Spatially Growing Disturbances in an Inviscid Shear Layer, *Journal of Fluid Mechanics*, **23** (3), 521–544.

Michalke, A. 1984 Survey On Jet Instability Theory, *Prog. Aerospace Sci.*, **21**, 159–199.

Myers, M. K. 1980 On the acoustic boundary condition in the presence of flow, *Journal of Sound and Vibration*, **71** (3), 429–434.

Peake, N. 1997 On the behaviour of a fluid-loaded cylindrical shell with mean flow, *Journal of Fluid Mechanics*, **338**, 387–410.

Peake, N. 2002 Structural Acoustics with Mean Flow, *Sound-Flow Interactions*, Y. Aurégan, A. Maurel, V. Pagneux, J.-F. Pinton (eds.), Springer-Verlag Berlin Heidelberg, 248–264.

Pridmore-Brown, D.C. 1958 Sound Propagation in a Fluid Flowing through an attenuating Duct, *Journal of Fluid Mechanics*, **4**, 393–406, 1958

Richter, C. 2009 *Liner impedance modeling in the time domain with flow*, Dissertation, Technische Universität Berlin.

Richter, C. Thiele, F. Li, X. & Zhuang, M. 2006 Comparison of Time-Domain Impedance Boundary Conditions by Lined Duct Flows, AIAA-2006-2527, *12th AIAA/CEAS Aeroacoustics Conference, 8-10 May 2006, Cambridge, MA*

Rienstra, S.W. & Darau, M. 2010 Mean Flow Boundary Layer Effects of Hydrodynamic Instability of Impedance Wall, *Proc. IUTAM Symposium on Computational Aero-Acoustics for Aircraft Noise Prediction, Southampton 2010*

Rienstra, S.W. & Tester, B.T. 2008 An Analytic Green's Function for a Lined Circular Duct Containing Uniform Mean Flow, *Journal of Sound and Vibration*, **317**, 994–1016.

Rienstra, S.W. & Vilenski, G.G. 2008 Spatial Instability of Boundary Layer Along Impedance Wall, AIAA-2008-2932, *14th AIAA/CEAS Aeroacoustics Conference, 5-7 May 2008, The Westin Bayshore Vancouver, Vancouver, Canada*

Rienstra, S.W. 2003 A Classification of Duct Modes Based on Surface Waves, *Wave Motion*, **37** (2), 119–135, 2003.

Rienstra, S.W. 2006 Impedance Models in Time Domain, including the Extended Helmholtz Resonator Model, AIAA-2006-2686, *12th AIAA/CEAS Aeroacoustics Conference, 8-10 May 2006, Cambridge, MA*.

Rienstra, S.W. 2007 Acoustic Scattering at a Hard-Soft Lining Transition in a Flow Duct, *Journal of Engineering Mathematics*, **59** (4), 451–475.

Tester, B.J. 1973 The Propagation and Attenuation of Sound in Ducts Containing Uniform or "Plug" Flow. *Journal of Sound and Vibration* **28**(2), 151–203.

Tester, B.J. 1973 Some Aspects of "Sound" Attenuation in Lined Ducts containing Inviscid Mean Flows with Boundary Layers. *Journal of Sound and Vibration* **28**(2), 217–245.

PREVIOUS PUBLICATIONS IN THIS SERIES:

Number	Author(s)	Title	Month
10-65	A. Hlod A.A.F. van de Ven M.A. Peletier	A model of rotary spinning process	Oct. '10
10-66	A. Hlod	On modeling of curved jets of viscous fluid hitting a moving surface	Oct. '10
10-67	A. Hlod J.M.L. Maubach	On error estimation in the fourier modal method for diffractive gratings	Oct. '10
10-68	J.H.M. Evers A. Muntean	Modeling micro-macro pedestrian counterflow in heterogeneous domains	Nov. '10
10-69	S.W. Rienstra M. Darau	Boundary layer thickness effects of the hydrodynamic instability along an impedance wall	Nov. '10

Ontwerp: de Tantes,
Tobias Baanders, CWI